Influence of medium-high frequency phase aberrations on 3ω focal spot in frequency tripling

Fang Wang (王 芳), Jingqin Su (粟敬钦), Wenyi Wang (王文义), Lanqin Liu (刘兰琴), Feng Jin (景 峰), and Xiaofeng Wei (魏晓峰)

Research Center of Laser Fusion, China Academy of Engineering Physics, Mianyang 621900

Quantitative analysis of frequency tripling based on the transform of phase aberrations is presented to study the influence of medium-high phase errors on focal spot tails. Nine-fold increase of energy fraction of high-order spectrum caused by the noises in the "waviness-1" regime would result in power growth of 3ω tails and significantly enlarge the spot size from 1ω to 3ω laser. The power growth in "waviness-1-2" regime (0.1−0.4 mm^{-1}) is with main responsibility for the increment of 3ω spot tails, as noises in whole "waviness-1" portion answer for the growth of 1ω spot tails. Theoretical predictions are shown to be consistent with numerical simulations on focal spot with variant phase ripples and different B-integral values.

OCIS code: 190.2620.

The inertial confinement fusion (ICF) mission has strict focus-ability requirements on driver at 0.351 μm output wavelength, and for example, in the national ignition facility (NIF) 95% of the power is required to be delivered inside a half-angle of 43 μrad[1]. Degradation of 3ω beam quality depends on 1ω laser aberrations and frequency transformation. Divergence associated with the 1ω laser has been well characterized through detailed studies[1−4]. Nevertheless, the issues that how aberrations of 1ω laser contribute to the 3ω focal spot in a complex manner in the frequency converter have not been well characterized yet. Auerbach *et al.* established a transfer theory to predict the transfer of small electric field ripples in frequency doubling and tripling, and found that a factor of 3 was gained in the magnitude of 1ω phase aberrations under close attainment of phase matching condition[5]. A multi-order diffractive model on focusing properties of harmonic beams was presented with the diamond-turned surfaces of the converter crystal[6]. Practically, nonlinear index of refraction could cause power growth of medium-high spatial frequency phase errors and intensity ripples. The ripples, in so-called "waviness-1" regime (NIF specification, from 0.03 to 0.4 mm^{-1}), which are not stopped by pinholes or occur after the last pinhole, would contribute to the increase of 3ω focal spot size. It is essential to understand the effects of noises in the waviness-1 regime on 3ω spot tails with an analytical model.

In this paper, quantitative analysis for the influence of medium-high phase errors on the tail of focal spot was presented. Then, based on the transform of phase aberrations in frequency tripling, detailed instructions on the power growth of 3ω spot tails from 1ω to 3ω laser were given. Full numerical simulations on focal spot with variant phase ripples and different B-integral values are conducted. The results confirmed the developed theories concerning the above factors. As a definition, in this paper, the tails of focal spot is the fraction enclosed inside a half-angle of 35 μrad according to the requirement of divergence specifications for ICF.

We develop an analytical theory to explain the spot tails quality variation with phase ripples in the waviness-1 regime. Wave front aberrations with random geometry can be represented by sum of sinusoidal series with different spatial frequencies[7]

$$\phi(x,y)=\sum_n[c_n(x,y)\sin(2\pi\xi_n x)+d_n(x,y)\sin(2\pi\eta_n y)], \tag{1}$$

where c_n and d_n are amplitudes of phase ripples, ξ_n and η_n are spatial frequency, and x and y are spatial coordinates. A simplified model of phase ripples was adopted when only one-dimensional model and single spatial frequency was considered, i.e.

$$\phi(x)=a\sin(2\pi\xi x). \tag{2}$$

The input electric field was assumed to be with ideal uniform and normalized amplitude

$$E(x)=\mathrm{e}^{-i\phi(x)}. \tag{3}$$

We obtained the Taylor expansion of Eq. (3) by weak phase distortion approximation, i.e., $|\phi(x)|\ll 1$, which could be satisfied easily for the medium-high components.

$$E(x)=1-ia\sin(2\pi\xi x)-\frac{a^2}{2}\sin^2(2\pi\xi x)+\frac{i}{6}a^3\sin^3(2\pi\xi x). \tag{4}$$

By Fourier transform for Eq. (4), far-field amplitude distribution is given by

$$E(f_x)=\left(1-\frac{a^2}{4}\right)\delta(f_x)\pm\left(\frac{a}{2}-\frac{a^3}{16}\right)\delta(f_x\pm\xi)+\frac{a^2}{8}\delta(f_x\pm 2\xi)\pm\frac{a^3}{48}\delta(f_x\pm 3\xi). \tag{5}$$

Thus we obtain the far-field intensity distribution in terms of orders of spatial spectrum

$$I(f_x)\propto|E(f_x)|^2=I_0(a)\delta(f_x)+I_N(a)\delta(f_x\pm N\xi), \tag{6}$$

where I_0 denotes zero-order spectrum and I_N denotes the Nth-order spectrum. Omitting the high-order compo-

nents greater than a^6 then we got I_0 and I_N $(N = 1, 2, 3)$:

$$I_0(a) = \left(1 - \frac{a^2}{4}\right)^2, \quad I_1(a) = \left(\frac{a}{2} - \frac{a^3}{16}\right)^2, \\ I_2(a) = \left(\frac{a^2}{8}\right)^2, \qquad I_3(a) = \left(\frac{a^3}{16}\right)^2. \tag{7}$$

Here we defined r_N as the energy fraction of Nth spectrum

$$r_N = I_N / I. \tag{8}$$

From Eq. (8) we could obtain energy fraction of all spectra. The fraction of high order spectra can be derived simply by sum of r_N,

$$r = \sum r_N \\ = \frac{\left(\frac{a}{2} - \frac{a^3}{16}\right)^2 + \left(\frac{a^2}{8}\right)^2 + \left(\frac{a^3}{48}\right)^2}{\left(1 - \frac{a^2}{4}\right)^2 + \left(\frac{a}{2} - \frac{a^3}{16}\right)^2 + \left(\frac{a^2}{8}\right)^2 + \left(\frac{a^3}{48}\right)^2}. \tag{9}$$

Since ripples in the waviness-1 regime contribute to the portion outside the 1ω main spot, we can also regard r as the fraction of spot tails. But for 3ω laser, it is more complex because lower-frequency portion is inside the main spot. Allowing for weak phase distortion, here we neglect the high-order terms, then a simple expression between spot tails and medium-high frequency ripples can be described as

$$r \approx a^2/4. \tag{10}$$

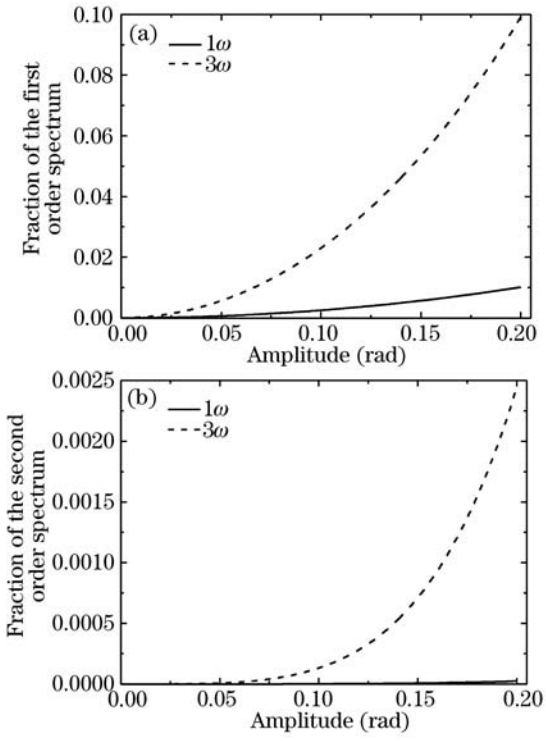

Fig. 1. Fraction of (a) first order and (b) second order spectrum versus the amplitude of phase ripples.

Obviously from Eqs. (7)−(9), r is a monotone increasing function of the phase ripple a, and r_N $(N > 2)$ is negligible compared with r_1, as indicated in Fig. 1.

According to ripple transfer theory[5], the transform of phase ripple from 1ω to 3ω is taken as

$$\varphi_{3\omega}(x, y) = 3\varphi_{1\omega}(x, y) + \alpha \Delta k \rho_{1\omega}, \tag{11}$$

where α denotes the coefficient associated with crystal length and conversion efficiency, δk and $\rho_{1\omega}$ are phase mismatching factor and amplitude perturbation of the input 1ω electric field, respectively. As mentioned above, the magnitude of 3ω phase aberrations is triple of 1ω field under the close attainment of phase matching condition. Nevertheless, actually, phase always mismatches in frequency converter, but δk and $\rho_{1\omega}$ are negligible in high efficiency frequency tripling, so on approximate triple relation for phase ripple transfer is attained in the analytical model

$$a_{3\omega} \approx 3a_{1\omega}. \tag{12}$$

We have constructed a simple wave-front model by adding a series of perturbation with different frequencies to an ideal uniform background field. The spatial wavelengths of these noises are in the waviness-1 regime and perturbation amplitudes are among 0 to 0.2 rad. According to the numerical model, Eqs. (9) and (11), the fraction of high-order spectra in 3ω field is about ninefold as in 1ω field (Fig. 2).

Nevertheless, because of the change in optical wavelength during tripling, the far-field divergence of 3ω beam shrinks to one-third of the 1ω beam, according to the definition of divergence angle,

$$\theta = \lambda \xi. \tag{13}$$

Thus, we have to divide the waviness-1 region into two parts, lower frequency portion (from 0.03 to 0.1 mm^{-1}, called "waviness-1-1") and higher frequency portion (from 0.1 to 0.4 mm^{-1}, called "waviness-1-2"). The first order spectrum of the former skips to main spot after tripling, so we can only consider effects of the second order spectrum. Therefore, the latter makes main contribution to 3ω spot tails. Herein, the 3ω beam divergence will be similar to that of the fundamental when the phase amplitudes in higher frequency portion are small.

We conduct focusing simulations on 1ω and 3ω fields with phase errors with different spatial wavelengths and perturbing amplitudes. The near-field distribution is assumed to be uniform, and the wavefront distortion is

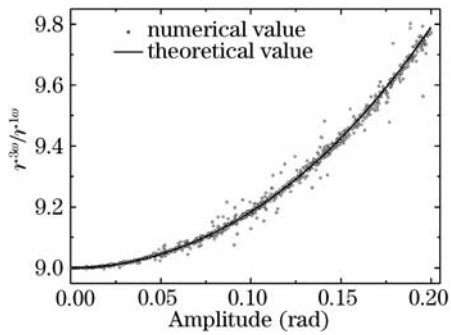

Fig. 2. High order spectra fraction ratio of 3ω field to 1ω field versus the amplitude of 1ω phase ripples.

constructed by add of the allowable amount in spatial frequency region. A Gaussian random phase screen models the low frequency portion "figure" (NIF specification, less than 0.03 mm^{-1})[2], and the "waviness-1" regions are constructed by the power spectrum density (PSD) restoring algorithm. This algorithm can produce an ensemble of equivalent wave fronts by choosing random phases in the Fourier domain and combining them with the given PSD-defined Fourier magnitude. Currently, higher frequency noises are not included in the model since they can be stopped by the pinhole. Generally, waviness regions are controlled by a PSD specification and the RMS specification is also introduced to choose the magnitude of phase ripples.

Plots in Fig. 3 show energy percent of focal spot tails with various phase errors. From Figs. 3(a) and (b), we can see that wavefront perturbation in "waviness-1-2" region has greater impact on the 3ω spot tails rather than 1ω spot tails. Additionally, there is little difference in the growth rate of tails energy percent between 1ω and 3ω spots when noises in "waviness-1-1" region increase. This is because that, noises of this portion cause the increment of tails energy by first-order spectrum in 1ω spot but second-order spectrum in 3ω spot, which have the same magnitude as discussed above. As can be seen from Figs. 3(c) and (d), contributions of phase aberrations in "figure" regime appear tiny on both 1ω and 3ω spot tails, unless the gradient root-mean-square (GRMS) of amplitudes becomes too big and causes the second-order spectrum of growth 1ω laser. The 1ω spot tails grow faster than 3ω with increasing of phase errors in "waviness-1-1" region. The 3ω spot size is smaller than 1ω spot when the amplitude of "waviness-1-1" region is negligible, resulted from the wavelength transform during in the tripling process. Thus, the power growth in "waviness-1-2" regime is with main responsibility for the increment of 3ω spot tails, as noises in whole "waviness-1" portion answer for the growth of 1ω spot tails.

The intensity dependent part of the refractive index of materials in the laser contributes to whole-beam and beam breakup, and causes power growth of medium-high frequency noises. B-integral is introduced to be the metric specifications for numerical studies, and it is defined as

$$B = \frac{2\pi}{2} \int \gamma I(z) \mathrm{d}z, \tag{14}$$

where γ denotes the nonlinear refractive index, $\sum B$ is the B-integral for the entire chain from beam injection to the input of frequency converter.

To study the influence of B-integral growth on 3ω spot quality, we conducted full simulations at different output powers. All studies were conducted with propagation codes SG99 and frequency conversion codes based on the nonlinear coupled wave equations. The model of frequency conversion includes the effects of nonlinear refraction index, linear loss, diffraction and walk-off, but no group velocity dispersion for its negligible effect to our case. Optical parameters and layout were taken from SGIII prototype facility. A 512×512, 41×41 (cm) grid was used for beam aperture of 29×29 (cm).

Results in Fig. 4 indicate that when $\sum B$ is small, such as 0.56 rad, the 1ω and 3ω focal spot sizes are of little difference, which is presented detailedly in reference[7]. The plots also show that the 1ω spot keeps almost constant with $\sum B$ for values from 0.56 to 6.27 rad, while the tails of 3ω spot grow rapidly. The threefold increase of phase

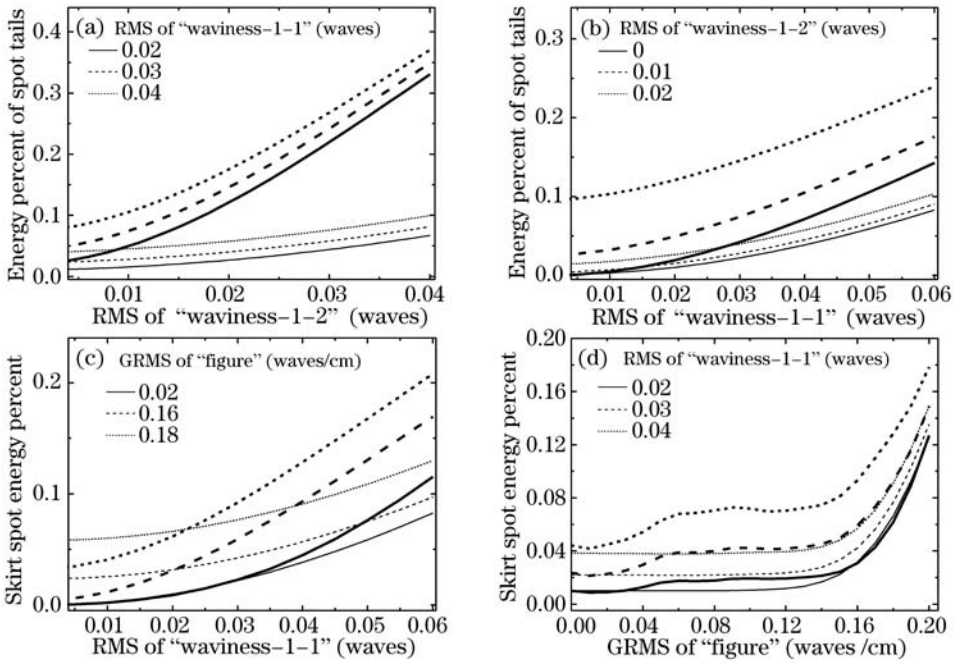

Fig. 3. Energy percent of focal spot tails for various phase aberrations of 1ω beam (thin curves) and 3ω beam (thick curves). Influence of phase noises in "waviness-1-1" and "waviness-1-2" regions on energy percent of spot tails are shown in (a) and (b) where the GRMS of "figure" is 0.1 waves/cm. Similarly, plots (c) and (d) show the effects of phase noises in "figure" and "waviness-1-1" region where the RMS of "waviness-1-2" is taken as zero.

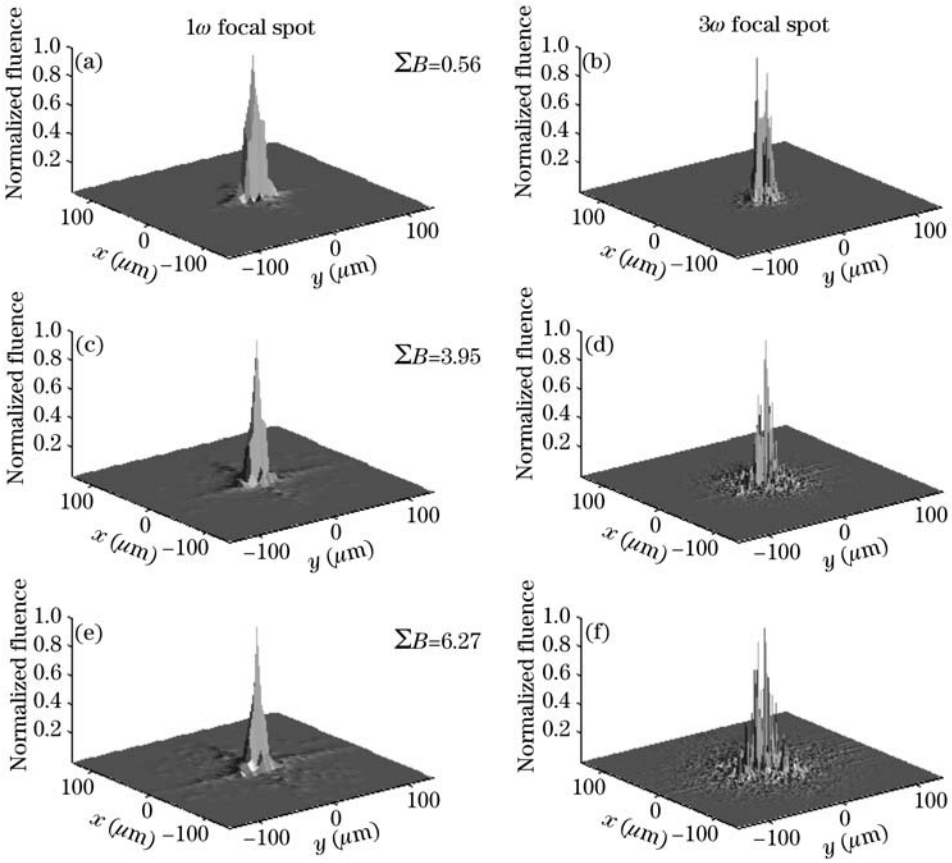

Fig. 4. Comparison of 1ω and 3ω focal spot size at different B-integral values.

gradient RMS leads to the degradation of 3ω focusing ability and 3ω focal spot would exhibit multiple-peak structure.

In conclusion, a quantitative analysis method was suggested for the influence of medium-high phase errors on the tail of focal spot. Based on the transform of phase aberrations in frequency tripling, energy fraction of overall high-order spectrums caused by the noises in the "waviness-1" regime increases by a factor of nine. Considering wavelength change in tripling, noises in "waviness-1-2" region make the most contribution to 3ω spot tails. The above conclusions were testified according to focusing model simulation by different RMS value of medium-high frequency ripples, as well as full numerical simulation at different system B-integral values.

F. Wang's e-mail address is wfoowf@yahoo.com.cn.

References

1. P. J. Wegner, J. M. Auerbach, C. E. Barker, S. C. Burkhart, S. A. Couture, J. J. DeYoreo, R. L. Hibbard, L. W. Liou, M. A. Norton, P. A. Whitman, and L. A. Hackel, UCRL-JC-129725 (1998).
2. J. K. Lawson, J. M. Auerbach, R. E. English, Jr., M. A. Henesian, J. T. Hunt, R. A. Sacks, J. B. Trenholme, W. H. Williams, M. J. Shoup III, J. H. Kelly, and C. T. Cotton, Proc. SPIE **3492,** 36 (1999)
3. W. Williams, J. Auerbach, J. Hunt, L. Lawson, K. Manes, C. Orth, R. Sacks, J. Trenholme, and P. Wegner, UCRL-JC-127297 (1997).
4. W. H. Williams, J. M. Auerbach, M. A. Henesian, J. K. Lawson, J. T. Hunt, R. A. Sacks, and C. C. Widmayer, Proc. SPIE **3264,** 93 (1998).
5. J. M. Auerbach, D. Eimer, D. Milam, and P. W. Milonni, Appl. Opt. **36,** 606 (1997).
6. T. Wang, T. Zhan, H. Zhu, and L. Qian, J. Opt. Soc. Am. B **19,** 1101 (2002).
7. W. H. Williams, J. M. Auerbach, M. A. Henesian, J. K. Lawson, P. A. Renard, and R. A. Sacks, Proc. SPIE **3492,** 55 (1999).
8. H. Liu, F. Jing, Y. Zuo, D. Hu, J. Su, Z. Peng, W. Zhou, Q. Li, and K. Zhang, Chin. J. Lasers (in Chinese) **33,** 504 (2006).